Applied Acoustics 116 (2017) 390–393

Contents lists available at ScienceDirect

Applied Acoustics

journal homepage: www.elsevier.com/locate/apacoust

Resonance switching in a large sonic crystal cavity

Alejo Alberti [a], Ignacio Spiousas [b], Pablo M. Gomez [c], Manuel C. Eguia [a,*]

[a] Laboratorio de Acústica y Percepción Sonora, Escuela Universitaria de Artes, CONICET, Universidad Nacional de Quilmes, B1876BXD Bernal, Argentina
[b] Laboratorio de Dinámica Sensomotora, Departamento de Ciencia y Tecnología, CONICET, Universidad Nacional de Quilmes, B1876BXD Bernal, Argentina
[c] Laboratorio de Acústica y Electroacústica, Universidad de Buenos Aires Av., Paseo Colón 850, C1063ACV Buenos Aires, Argentina

ARTICLE INFO

Article history:
Received 3 August 2016
Received in revised form 11 October 2016
Accepted 18 October 2016
Available online 25 October 2016

Keywords:
Sonic crystal
Resonance
Switching
Metamaterial

ABSTRACT

In this work we present an experimental realization of resonance switching inside a large, relative to the lattice constant, sonic crystal (SC) cavity. The resonances arise from a temporary trapping of the acoustical energy between two sonic crystal slabs when the frequency of the wave falls within a partial band-gap region (thus, the propagation inside the sonic crystal is inhibited for normal incidence and a total reflection occurs). We show that by modifying the geometry of the sonic crystal lattice, from square to centered rectangular, it is possible to switch some resonances on and off, for a certain frequency region corresponding to the second band-gap for normal incidence. We also study the generalization of this phenomenon for the same lattice and band-gap region, as a function of the length of the cavity and the filling fraction the lattice.

1. Introduction

Acoustic wave propagation in periodic composite materials, *i.e.*, sonic crystals (SCs), has attracted substantial attention during the last two decades. A SC consists of a periodic lattice of acoustic scatterers embedded in a background acoustic medium. This particular structure exhibits many remarkable properties, such as the existence of forbidden frequency ranges (band-gaps) [1], negative refraction [2], birefraction [3], and self-collimation [4], that can lead to applications ranging from sound barriers [5] to acoustic lenses [4] and energy harvesters [6]. Further, as the acoustic properties of the SCs depend solely on their geometric parameters, changes in the shape of the two dimensional lattice or of the scatterers can lead to changes in their acoustical properties.

In this way, tunable SCs could be devised, leading to potential technological applications. Different realizations of tunable SCs with variable geometry have been proposed so far, including rotating rods [7–10], tubular cylindrical inclusions [11], magnetoelastic [12] and elastomeric materials [13]. However, in these applications only transmission properties were exploited, while reflective properties, in contrast, remain less studied [14,15]. It has been shown that incident acoustic waves with frequencies within the band-gap region are totally reflected back, since propagation inside the sonic crystal is inhibited [14]. This kind of reflection is observed both for full band-gaps (the propagation inside the SC is inhibited for all incidence angles) and partial band-gaps (the propagation is inhibited only for a range of incidence angles).

Also, the possibility of devising a SC resonant cavity using the band-gap total reflection has been recently proposed both theoretically [16] and experimentally [17]. In Spiousas et al. [16] it was further proposed that the resonances of the cavity can be tuned by changing the geometry of the SC lattice.

The resonances in the SC cavity arise from the interplay between the frequency and angular-dependent reflectivity of the sonic crystal and the geometry of the cavity. As it was shown in Alberti et al. [17], the total reflection of the acoustical waves for all angles of incidence that occurs within the full band-gap frequency region gives rise to axial and tangential modes (as would occur in an ordinary two-dimensional cavity) but also to other 'exotic' modes for which the SC wall and the cavity cannot be decoupled.

The fact that the occurrence of many of these resonances can be modified (tuned or switched on and off) by changing the geometry of the SC lattice only, without changing the cavity dimensions, makes the modal analysis of a sonic crystal cavity an interesting subject for study.

In this work, we will study the simplest realization of resonance switching within a SC cavity, formed by two parallel SC walls and an (almost) planar transducer in between. The SCs are made by a two-dimensional array of rigid cylinders. In this way, we intend to advance in the understanding of the modal structure of the cavity, through comparisons with theoretical models and modifica-

* Corresponding author.
E-mail addresses: alejo.alberti@lapso.org (A. Alberti), ispiousas@unq.edu.ar (I. Spiousas), pgomez@fi.uba.ar (P.M. Gomez), meguia@unq.edu.ar (M.C. Eguia).

http://dx.doi.org/10.1016/j.apacoust.2016.10.016
0003-682X/

tions on the geometry of the SC walls. In particular, we will concentrate on a normal-incidence partial band-gap for which the axial modes can be switched on and off by displacing rows of cylinders. Even when the tuning requires a physical contact with the sample, it is probably one of the clearest implementations of resonance switching of mechanical waves, achievable by simple means.

2. Apparatus and methods

The experimental setup consisted of two SC slabs (13×6 cylinders each, with radii of 1.27 cm and lattice constant $a = 3.33$ cm) placed parallel and 59 cm apart from each other. The SC cavity was mounted inside a wooden box covered by sound-absorbing panels (pyramid polyurethane acoustical foam, 35 mm). In Fig. 1a we display the box with the top plate removed. Since we are studying frequencies above 3 kHz, the absorption coefficients of the walls are all above 0.97 (data provided by the manufacturer). A custom-made plane ionic transducer (21.5 cm wide $\times$ 30 cm high) [18] placed in the middle of the box was used as the acoustic source. Due to its constructive characteristics, the transducer emits roughly-plane wavefronts and operates effectively as a volume velocity source with both monopolar and dipolar components, allowing it to excite modal resonances both with zero and maximum particle displacement at its center.

The acoustic field inside the cavity was recorded using a microphone (Brüel & Kjær type 4133) inserted through the top plate of the box with its capsule located at half height of the ionic transducer. Measurements were made along a central line perpendicular to the SC slabs (yellow dashed line in Fig. 1a), covering distances to the source between 3 and 25 cm in 100 equal steps. We also made measurements along ten lines parallel to the central measurement line, up to 5 cm away in both directions. We checked that no noticeable differences were found between the results obtained from different lines, and therefore in the following we will refer only to results obtained from the central line.

Measurements were made for two different geometries of the SC walls: square lattice ('null-displacement' condition, d_0, Fig. 1b) and centered rectangular lattice ('maximum-displacement' condition, d_{max}, Fig. 1c). This last condition is obtained from the square lattice by displacing one every two rows a distance of $a/2$. The band diagrams associated with each geometry are displayed in Fig. 1d and e, along with the frequency regions covered by the total (dark gray) and partial (light gray) band-gaps studied in this letter. As it can be seen from the Figure, the null-displacement condition exhibits two band-gaps (BG): a full one ranging from 5.41 to 6.50 kHz and a partial one covering from 8.37 to 10.43 kHz. For the maximum displacement condition the total BG remains almost unchanged while the partial BG vanishes.

3. Results and discussion

Fig. 2 summarizes the results obtained from the experimental measurements for the (a) null-displacement and (b) maximum-displacement conditions. The vertical axis corresponds to the distance from the source to the measuring points along the central line (see Fig. 1a), and the horizontal axis spans the frequency range of interest, from 3 to 11 kHz. The color scale represents sound pressure in dB in arbitrary units. For the first configuration (null-displacement) two groups of resonances can be identified, covering frequencies corresponding to a full (from 3 to 6.5 kHz, approximately) or partial (roughly from 8 to 10 kHz) BG, as can be seen from the band diagram (Fig. 1d). However, while the lower frequency resonances remains in the displaced configuration, those resonances corresponding to the partial BG are absent. This is consistent with the band diagram for the centered rectangular lattice (Fig. 1e).

In order to compare these results with the theoretical predictions, we carried out numerical simulations of an equivalent two-dimensional system employing the multiple-scattering theory (MST) method. Upon calculating the acoustic field in the same spatial and spectral regions covered by the measurements, the sound pressure level (SPL) was averaged along the central line. This magnitude is displayed in Fig. 2c and d with blue (color online) lines. As a comparison, we display the same magnitude obtained from

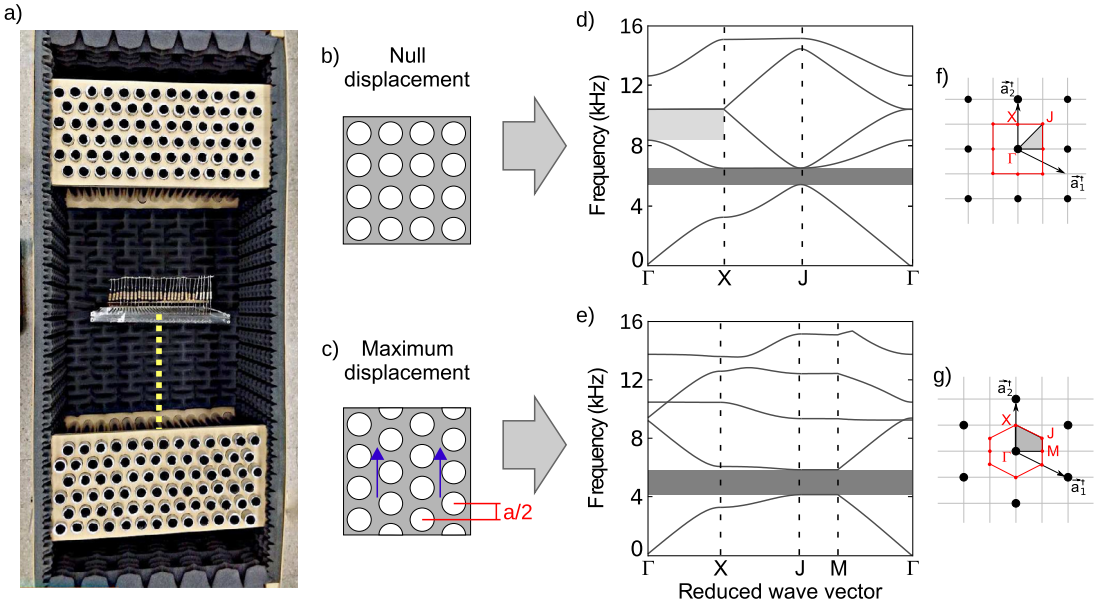

Fig. 1. (a) Plan view of the cavity under study, showing two parallel SC slabs and a plane acoustic transducer between them. The yellow dotted line corresponds to the measurement points. (b) and (c) display schematically the geometries of the lattices explored (null and maximum displacement of cylinders, corresponding to square and centered rectangular lattices, respectively) and (d) and (e) their corresponding bang diagrams. Regions painted in light (dark) gray indicate the presence of a partial (total) band gap. (f) and (g) provide details of the corresponding irreducible Brillouin zones and basis vectors. (For interpretation of the references to colour in this figure legend, the reader is referred to the web version of this article.)

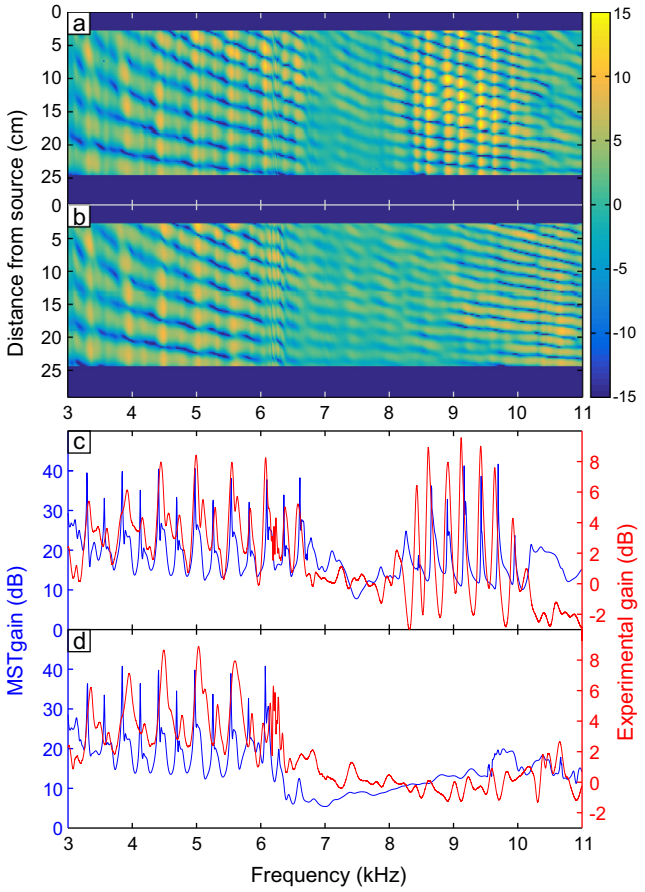

Fig. 2. Measured sound pressure level for (a) the null and (b) maximum displacement conditions for the sonic crystal cavity described in Fig. 1, as a function of frequency and distance from the source. Average sound pressure levels from experiments (red line) and numerical calculations (blue line) are displayed for (c) null displacement and (d) maximum displacement conditions. (For interpretation of the references to colour in this figure legend, the reader is referred to the web version of this article.)

experimental data in red (color online) lines, which offers a good correspondence with the theoretical results both in terms of peaks localization and relative amplitude. The most substantial result is the vanishing of the resonances corresponding to the partial band gap region when the d_{max} configuration is adopted, something which stands out both in the experimental and theoretical data.

The fact that some resonances can be 'turned off' via a simple manipulation of the lattice geometry enables the system to function as an acoustic switching mechanism. In order for this mechanism to be effective, a number of modal resonances should be contained in the BG for one configuration and not for the other one. This fact sets the basic design rules for such a device. First, the 'center' and width of the normal incidence BG have to be determined by setting the lattice constant (a) and the ratio between the radius and the lattice constant (r/a), i. e. the filling fraction of the lattice [19], respectively; and second, the amount of modal frequencies falling in that frequency range has to be determined by adjusting the distance between walls (L).

Then, to assess the robustness and generality of this phenomenon, we employed MST for exploring the behavior of this device for a parameter space defined by the normalized separation between the walls (L/a) and the normalized radii of the cylinders (r/a). The ranges of values explored were $4.55 < L/a < 27.44$ and $0.20 < r/a < 0.47$ (the values corresponding to the experimental setup are $L/a = 8.86$ and $r/a = 0.38$).

In this context, we proceeded to determine the existence of switching following these criteria: if at least one resonance could be found for d_0 while d_{max} showed none, then we considered 'total' switching; if both configurations displayed peaks but the amount for d_0 was at least three times higher than for d_{max}, then we considered 'partial' switching. A resonance was considered whenever a local maximum of the average SPL was higher than 22 dB and with a prominence of at least 4 dB relative to its neighboring peaks (as implemented in the findpeaks.m MATLAB® function).

The contour map in Fig. 3a represents the number of resonances on the second normal-incidence BG for the d_0 configuration, found through the numerical procedure described before, as a function of L/a and r/a. For the parameters space explored, the number of peaks ranged from 0 to 12. The regions for 'total' (darker shaded area) and 'partial' (lighter shaded area) switching effect, according to the criteria defined before, appear overprinted on this figure. Furthermore, the regions defined here give us a complete description of what combination of cylinder radius and wall separation, for a given lattice constant, allows the device to maximize the switching effect. For example, for $r/a = 0.4$ and $L/a = 16$ the device would allow seven resonances for the d_0 condition while no resonances are allowed for the d_{max} condition.

In Fig. 3b and c we show an example of the switching behavior for $L/a = 16$. In these figures the vertical axis still represents r/a while the horizontal axis now corresponds to the normalized frequency λ/a, and the color code for the average SPL in dB. Fig. 3b and c correspond to this diagram for the d_0 and d_{max} conditions, respectively, and the resonances are marked with a black dot. Solid black lines delimit the normal-incidence BG regions as obtained from the plane wave expansion method. As can be seen, the BG region width for $r/a = 0.4$ becomes narrower making the number

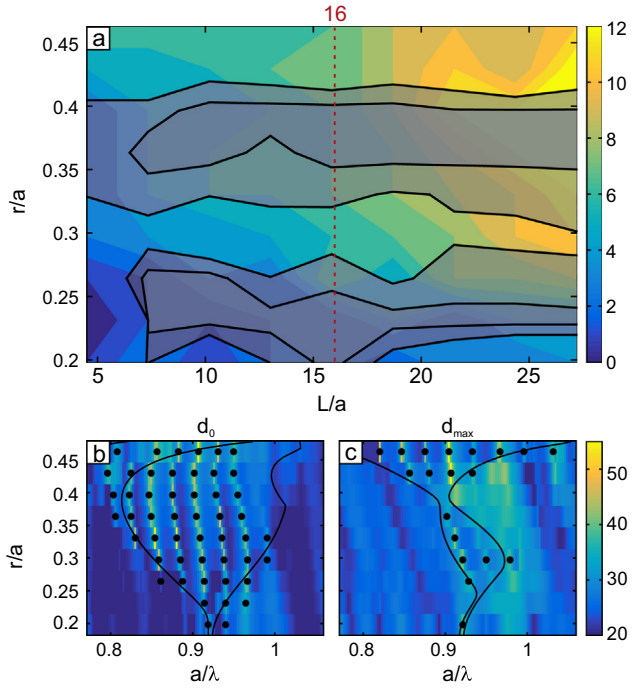

Fig. 3. (a) Representation of the parameter space regions where the switching effect occurs, either totally (inner gray regions) or partially (outer gray regions). The color scale represents the amount of resonances present for each $(L/a, r/a)$ pair, for the d_0 configuration. As an example (b) and (c) display the locations of the observed resonances (black dots) for $L/a = 16$ for each value of r/a, for maximum and null displacements, respectively. Dark lines demarcate normal incidence band gap regions calculated using plane wave expansion, within which the resonances are expected to be observed. (For interpretation of the references to colour in this figure legend, the reader is referred to the web version of this article.)

of resonances contained within that region to shift from seven to zero, enabling the device to work as a 'total' acoustic switch, as predicted in Fig. 3a.

4. Conclusions

A cavity with sonic crystal walls was built in order to study its modal behavior. Upon obtaining the transfer function of the system we observed that it effectively operates as a band pass filter, trapping between the walls the acoustic waves with frequencies falling into a band gap and permitting the dissipation of the remaining stimuli through the borders. The modal behavior was thus found to be the combination of two factors: those resonances corresponding to modal frequencies according to the characteristic distance between the walls and the amplitude modulation introduced on them by the sonic crystal slabs. After studying the responses for two different types of sonic crystals (square and centered rectangular lattices) we found that a set of modal frequencies corresponding to a partial BG disappeared for the second case, thus suggesting the possibility of implementing a geometry-based acoustic switch. We explored the space parameter that characterizes the system finding those geometrical parameters which optimize the desired effect. This implementation can be used as a configurable band pass filter in analog acoustic circuitry or as a possible approach towards logic gates in digital acoustic circuitry programming.

References

[1] Martínez-Sala R, Sancho J, Sánchez JV, Gómez V, Llinares J, Meseguer F. Nature 1995;378:241.
[2] Zhang X, Liu Z. Appl Phys Lett 2004;85:341.
[3] Lu M-H, Zhang C, Feng L, Zhao J, Chen Y-F, Mao Y-W, et al. Nature Mat 2007;6:744.
[4] Chen L-S, Kuo C-H, Ye Z. Appl Phys Lett 2004;85:1072.
[5] Sánchez-Perez JV, Rubio C, Martinez-Sala R, Sánchez-Grandia R, Gomez V. Appl Phys Lett 2002;81:5240.
[6] Wu L-Y, Chen L-W, Liu C-M. Appl Phys Lett 2009;95:013506.
[7] Goffaux C, Vigneron J. Phys Rev B 2001;64:075118.
[8] Wu F, Liu Z, Liu Y. Phys Rev E 2002;66:1.
[9] Pichard H, Richoux O, Groby J-P. J Acoust Soc Am 2012;132:2816.
[10] Romero-García V, Lagarrigue C, Groby J-P, Richoux O, Tournat V. J Phys D: Appl Phys 2013;46:305108.
[11] Khelif A, Deymier PA, Djafari-Rouhani B, Vasseur JO, Dobrzynski L. J Appl Phys 2003;94:1308.
[12] Robillard JF, Matar OB, Vasseur JO, Deymier PA, Stippinger M, Hladky-Hennion aC, et al. Appl Phys Lett 2009;95:3.
[13] Yang W-P, Wu L-Y, Chen L-W. J Phys D: Appl Phys 2008;41:135408.
[14] Sanchis L, Cervera F, Sánchez-Dehesa J, Sánchez-Perez JV, Rubio C, Martinez-Sala R. J Acoust Soc Am 2001;109:2598.
[15] Sanchis L, Håkansson A, Cervera F, Sánchez-Dehesa J. Phys Rev B 2003;67:035422.
[16] Spiousas I, Eguia MC. J Acoust Soc Am 2012;132:2842.
[17] Alberti A, Gomez PM, Spiousas I, Eguia MC. Appl Acoust 2016;104:1.
[18] Gomez MP, D'Onofrio E, Santiago G. IEEE Lat Am Trans 2015;13(3):578.
[19] Rubio C, Caballero D, Sanchez-Perez JV, Martinez-Sala R, Sanchez-Dehesa J, Meseguer F, et al. J Light Technol 1999;17(11):2202.